arXiv:1203.5441v1 [astro-ph.EP] 24 Mar 2012

K-shell photoionization of ground-state Li-like carbon ions [C^{3+}]: experiment, theory and comparison with time-reversed photorecombination

A Müller[1], S Schippers[1], R A Phaneuf[2], S W J Scully[2,3], A Aguilar[2,4], A M Covington[2], I Álvarez[5], C Cisneros[5], E D Emmons[2], M F Gharaibeh[2]†, G Hinojosa[5], A S Schlachter[4] and B M McLaughlin[3,6]‡

[1]Institut für Atom-und Molekülphysik, Justus-Liebig-Universität Giessen, 35392 Giessen, Germany
[2]Department of Physics, University of Nevada, Reno, Nevada 89557, USA
[3]School of Mathematics and Physics, The David Bates Building, 7 College Park, Queen's University Belfast, Belfast BT7 1NN, UK
[4]Lawrence Berkeley National Laboratory, Berkeley, California 94720, USA
[5]Centro de Ciencias Físicas, Universidad Nacional Autónoma de México, Apartado Postal 6-96, Cuernavaca 62131, Mexico
[6]Institute of Theoretical Atomic and Molecular Physics, Harvard Smithsonian Center for Astrophysics, MS-14, Cambridge, Massachusetts 02138, USA

Abstract. Absolute cross sections for the K-shell photoionization of ground-state Li-like carbon [$C^{3+}(1s^2 2s\ ^2S)$] ions were measured by employing the ion-photon merged-beams technique at the Advanced Light Source. The energy ranges 299.8–300.15 eV, 303.29–303.58 eV and 335.61–337.57 eV of the $[1s(2s2p)^3P]^2P$, $[1s(2s2p)^1P]^2P$ and $[(1s2s)^3S\ 3p]^2P$ resonances, respectively, were investigated using resolving powers of up to 6000. The autoionization linewidth of the $[1s(2s2p)^1P]^2P$ resonance was measured to be 27±5 meV and compares favourably with a theoretical result of 26 meV obtained from the intermediate coupling R-Matrix method. The present photoionization cross section results are compared with the outcome from photorecombination measurements by employing the principle of detailed balance.

PACS numbers: 32.80.Fb, 31.15.Ar, 32.80.Hd, and 32.70.-n

Short title: K-shell photoionization of C^{3+} ions
Submitted to J. Phys. B: At. Mol. & Opt. Phys: 1 March 2013

† Present address: Department of Physics, Jordan University of Science and Technology, Irbid, 22110, Jordan
‡ Corresponding author, e-mail: b.mclaughlin@qub.ac.uk

1. Introduction

The *Chandra* and the *XMM-Newton* satellites are currently providing a wealth of x-ray spectra on many astronomical objects. There is a serious lack of adequate atomic data, particularly in the K-shell energy range, needed for the interpretation of these spectra. Spectroscopy in the soft x-ray region (5-45 Å), including K-shell transitions for singly, doubly and triply charged ionic forms of atomic elements such as; C, N, O, Ne, S and Si, and the L-shell transitions of Fe and Ni, provide a valuable probe of the extreme environments in active galactic nuclei (AGN's), x ray binary systems, and cataclysmic variables [1]. The goal of the present investigation is to provide accurate values for photoionization cross sections, resonance energies, and autoionization linewidths resulting from the photoabsorption of x rays near the K-edge of Li-like carbon.

The synergistic and symbiotic relationship between theoretical and experimental studies is essential to verify the data produced from such investigations. Identification of Auger states from multiply charged ionic states of carbon have been performed experimentally by Schneider and co-workers [2]. Excitation energies of several autoionizing states in the C^{3+} ion were determined by Hofmann *et al* [3] by using collisional spectroscopy of fine details in the cross section for electron impact ionization of C^{3+} ions. Jannitti and co-workers [4] were the first to measure photoionization (PI) cross sections for this Li-like carbon ion over a wide range of energies using the dual laser plasma (DLP) technique at low spectral resolution compared to the present study. Recently, extremely high resolution measurements for K-shell photoexcitation of singly and doubly charged ions of carbon have been carried out within our international collaboration; C^{+} [5] and C^{2+} [6]. Such studies are important in order to provide accurate results for absolute photoionization cross sections, resonance energies and autoionization linewidths. These benchmarked results therefore update existing literature values [7, 8, 9, 10] and as such should be used in preference to those that are currently in use in the various astrophysical modelling codes such as CLOUDY [11, 12] and XSTAR [13].

The present study aims to benchmark theoretical values for PI cross sections, resonance energies and lifetimes of autoionizing states of the C^{3+} ion in the vicinity of the K-edge with high-resolution experimental measurements. This provides confidence in the data that may be used in modelling astrophysical plasmas; e.g., in the hot (photoionized and collisionally ionized) gas surrounding ζ Oph [14] where C IV has been observed in absorption or for the non-LTE modelling of early B-type stars [15].

Promotion of a K-shell electron in Li-like carbon (C^{3+}) ions to an outer np-valence shell ($1s \rightarrow np$) from the ground state produces states that can autoionize, forming a C^{4+} ion and an outgoing free electron via the processes;

$$h\nu + C^{3+}(1s^2 2s) \rightarrow C^{3+}\ (1s2snp,\ n = 2, 3, 4 \ldots)$$

$$\downarrow$$

$$C^{4+}\ (1s^2) + e^{-}.$$

The strongest excitation process in the interaction of a photon with the $1s^2 2s\ {}^2S$ ground-state of the Li-like carbon ion is the $1s \rightarrow 2p$ photo-excitation process producing intermediate doubly excited C^{3+} ($[1s\,(2s\,2p)^3P]^2P^o$) and C^{3+} ($[1s\,(2s\,2p)^1P]^2P^o$). At higher energy $1s \rightarrow 3p$ photo-excitation processes produce C^{3+} ($[(1s2s)^3S\ 3p]\ {}^2P^o$). The inner-shell autoionization resonances created by the above

processes appear in the corresponding photoionization cross sections (in the energy region near to the K-edge) on top of a continuous background cross section for direct photoionization of the outer 2s electron. Indirect and direct photoionization channels can interfere with one another and produce asymmetric (Fano-Beutler) line profiles. Time-reversed C^{3+} photoionization processes described by equation (1) constitute contributions to dielectronic recombination of C^{4+}

The present investigation provides absolute values (experimental and theoretical) for photoionization cross sections, resonance energies and autoionization linewidths of the first three intermediate states formed by ($1s \rightarrow np$) photoexcitation of C^{3+}. In the ALS experiments, energy scan measurements were taken by stepping the photon energy through a preset range of values. The energy scan ranges were 299.8–300.15 eV, 303.29–303.58 eV (at a photon energy spread of $\Delta E = 46$ meV) and 335.61–337.57 eV (at $\Delta E = 121$ meV) and include the $[1s\,(2s\,2p)^3P]^2P^o$, $[1s\,(2s\,2p)^1P]^2P^o$ and $[(1s\,2s)^3S\ 3p]^2P^o$ resonances, respectively. The theoretical photoionization cross section was convoluted with a Gaussian of the same full-width at half maximum (FWHM) to simulate the energy resolution of the experiment, so that direct comparisons may be made with the measurements performed in the various energy regions. Such a comparison of theoretical and experimental results serves as an indication of the level of accuracy reached by the measurements and by the theoretical approach [16, 17].

The principle of detailed balancing can be used to compare the present PI cross-section measurements with previous experimental and theoretical cross sections for the time-inverse photo-recombination (PR) processes. This comparison provides a valuable check between entirely different experimental approaches for obtaining atomic cross sections on absolute scales. To benchmark theory and obtain suitable harmony with the present high-resolution photoionization experimental measurements performed at third-generation synchrotron light facilities (such as the Advanced Light Source), state-of-the-art theoretical methods are required using highly correlated wavefunctions [18, 19]. Additional theoretical calculations are usually required to determine the contribution from ions in metastable states which may be present in the parent ion beam (which is not an issue in the present case with Li-like ions). These features have been illustrated vividly from experimental and theoretical photoionization studies undertaken by our international collaboration, on a number of simple and complex ions. All of the experimental work was performed at the Advanced Light Source (ALS), in Berkeley, California for a variety of ions, e.g. He-like Li^+ [20, 21]; Be-like C^{2+} [22, 23], B^+ [24], C^{2+}, N^{3+} and O^{4+} [25]; B-like C^+ [5]; F-like Ne^+ [26]; N-like O^+ [27, 28], F^{2+} and Ne^{3+} [29]. The majority of these high resolution experimental studies from the ALS have been shown to be in excellent accord with detailed theoretical calculations performed using the state-of-the-art R-matrix method [30, 31].

No metastable ions were present in the Li-like C^{3+} ion beam in the current study. Photoabsorption experiments in the K-shell region have been performed elsewhere on this Li-like carbon ion species at lower resolution than the present experiment using the dual laser plasma (DLP) technique [4]. The DLP measurements have been very useful for obtaining absorption spectra over a wide energy range. However their interpretation can be complicated due to ions being distributed over various charge states in both the ground and metastable states, and the presence of a plasma can affect energy levels.

The layout of this paper is as follows. Section 2 presents a brief outline of

the theoretical work. Section 3 details the experimental procedure used. Section 4 presents a discussion of the results obtained from both the experimental and theoretical methods. Finally in section 5 conclusions are drawn from the present investigation.

2. Theory

Theoretical cross-section calculations for the photoionization of triply charged carbon ions are available from the Opacity Project and can be retrieved from the TOPBASE database [32]. These cross-section calculations primarily cover the valence region only and have been determined in LS-coupling. Theoretical results from the independent particle model exist in the energy region of the K-edge [8, 9, 10], but do not account for resonance effects that have been observed in the dual-laser-plasma (DLP) experimental work of Jannitti and co-workers or in the present study. Early R-matrix studies for the K-edge region of this ion were limited to LS-coupling [33] with no relativistic or radiation damping effects included in that work. No determination of resonance parameters were made in that early R-matrix work } but suitable agreement was found for the background cross section with the experimental work of Jannitti and co-workers [4, 33] and the independent particle model [8, 9, 10]. Recent studies by Pradhan and co-workers [34, 35] for K-shell photoionization cross sections on Li-like complexes have been obtained in intermediate coupling (primarily for astrophysical applications) with identification and determination of resonance parameters that will be discussed later in the paper.

The present investigation extends the earlier LS theoretical work on the C^{3+} ion [33], to include relativistic and radiation damping effects. Photoionization cross-section calculations for C^{3+} ions were performed both in LS and intermediate coupling. The intermediate coupling calculations were carried out using the semi-relativistic Breit-Pauli approximation which allows for relativistic effects to be included. Radiation-damping [36] effects were also included within the confines of the R-matrix approach [30, 31] for completeness. Relativistic effects need to be included when the experimental resolution is such that fine-structure effects can be resolved and radiation damping affects the narrow resonances present in the PI cross sections. An appropriate number of C^{4+} states (19 LS, 31 LSJ levels) were included in our intermediate coupling calculations. An n=4 basis set of C^{4+} orbitals was used which were constructed using the atomic-structure code CIV3 [37] to represent the wavefunctions. Photoionization cross-section calculations were then performed both in LS and intermediate coupling for the $1s^2 2s\ ^2S_{1/2}$ initial state of the C^{3+} ion in order to gauge the importance of including relativistic effects. The photoionization cross-section calculations were also performed with and without radiation damping in order to quantify this effect in the appropriate PI and PR cross sections. It turns out that only the narrow resonances in the appropriate cross sections are affected by radiation damping.

In the calculations the following He-like LS states were retained: $1s^2\ ^1S$, $1sns\ ^{1,3}S$, $1snp\ ^{1,3}P^\circ$, $1snd\ ^{1,3}D$, and $1snf\ ^{1,3}F^\circ$, $n \leq 4$, of the C^{4+} ion core which give rise to 31 LSJ states in the intermediate close-coupling expansions for the J=1/2 initial scattering symmetry of the Li-like C^{3+} ion. The use of the n=4 pseudo states is to attempt to account for correlations effects and the infinite number of states (bound and continuum) left out by the truncation of the close-coupling expansion in our work. For the structure calculations of the C^{4+} ion, all physical orbitals were included up to n=3 in the configuration-interaction wavefunctions expansions used to describe the

states.

The Hartree-Fock 1s and 2s orbitals of Clementi and Roetti [38] together with the n=3 orbitals were determined by energy optimization on the appropriate spectroscopic state using the atomic structure code CIV3 [37]. The n=4 correlation (pseudo) orbitals were determined by energy optimization on the ground state of this ion. All the states of the C^{4+} ion were then represented by using multi-configuration interaction wave functions. The Breit-Pauli R-matrix approach was used to calculate the energies of the $C^{4+}(LSJ)$ states and the subsequent photoionization cross sections. A minor shift (< 0.1 %) of the theoretical energies to experimental values [39] was made so that they would be in agreement with available experimental thresholds. Photoionization cross sections out of the C^{3+} ($1s^2 2s\ ^2S_{1/2}$) ground-state were then obtained for total angular momentum scattering symmetries of J = 1/2 and J= 3/2, odd parity, that contribute to the total.

The R-Matrix method [30, 31, 36] was used to determine all the photoionization cross sections for the initial ground state in LS and intermediate-coupling. The scattering wavefunctions were generated by allowing all possible three-electron promotions out of the base $1s^2 2s$ configuration of C^{3+} into the orbital set employed. Scattering calculations were performed with twenty-five continuum functions and a boundary radius of 8.4 Bohr radii. For the $^2S_{1/2}$ initial state the outer region electron-ion collision problem was solved (in the resonance region below and between all the thresholds) using a suitably chosen fine energy mesh of 10^{-7} Rydbergs ($\approx$ 1.36 μeV) to fully resolve all the extremely fine resonance structure in the appropriate photoionization cross sections. The QB technique (applicable to atomic and molecular complexes) of Berrington and co-workers [40, 41, 42] was used to determine the resonance parameters and averaging was performed over final total angular momentum J values. Finally, in order to compare directly with experiment, the theoretical cross section was convoluted with a Gaussian function of appropriate width to simulate the energy resolution of the measurement.

3. Experiment

The experiment was performed at the ion-photon-beam (IPB) end-station [26] of the undulator beamline 10.0.1 at the Advanced Light Source (located at the Lawrence Berkeley National Laboratory, in Berkeley, California, USA). The experimental method employed is similar to that first used by Lyon and co-workers [43] and in our earlier measurements of the K-shell PI cross sections for the C^{2+} ion [6].

C^{3+} ions were generated from CH_4 gas inside a compact all-permanent-magnet electron-cyclotron-resonance (ECR) ion source [44]. Collimated $^{12}C^{3+}$ ion-beam currents of typically 40 nA were extracted by placing the ion source at a positive potential of +6 kV and a dipole magnet selected ions of the desired ratio of charge to mass. In addition to $^{12}C^{3+}$, the selected ion beam contained other ions with nearly the same charge-to-mass ratio, such as $^{16}O^{4+}$ and $^4He^+$. The fraction of the measured ion current that was due to $^{12}C^{3+}$ was determined to be 87% from a separate measurement of the uncontaminated $^{13}C^{3+}$ ion beam current and applying the known $^{13}C/^{12}C$ natural isotopic abundance ratio of 0.01122. This correction to the measured primary ion beam current was applied to cross-section measurements.

The ion beam was placed onto the axis of the counter-propagating photon beam by applying appropriate voltages to several electrostatic ion-beam steering and focusing devices. Downstream of the interaction region, the ion beam was deflected out of the

photon beam direction by a second dipole magnet that also separated the ionized C^{4+} product ions from the C^{3+} parent ions. The C^{4+} ions were counted with a single-particle detector of nearly 100% efficiency, and the C^{3+} ion current was monitored for normalization purposes. The measured C^{4+} count rate was only partly due to photoionization events. It also contained C^{4+} ions produced by electron-loss collisions of C^{3+} ions in the parent beam with residual gas molecules and surfaces. For the determination of absolute cross sections this background was subtracted by time modulation (mechanical chopping) of the photon beam.

Absolute cross sections were obtained by normalizing the background-subtracted C^{4+} count rate to the measured ion current, to the photon flux, which was measured with a calibrated photodiode, and to the beam overlap. Beam overlap measurements were carried out using two commercial rotating-wire beam-profile monitors and a movable slit scanner. Due to the considerable effort required for carrying out reliable absolute cross-section measurements, these were performed at only a few selected photon energies in the vicinities of the resonance maxima. The systematic error of the absolute cross-section determination is estimated to be ± 20 % for the first two resonances. For the third resonance the efficiency of the photodiode was linearly extrapolated from the lower-energy behaviour adding 10 to 20 % uncertainty to the size of the $[(1s\,2s)^3S\ 3p]^2P^o$ peak.

Previous recombination storage-ring measurements made at the CRYRING [45, 46] and the current theoretical calculations guided the high-resolution energy scan measurements to be taken by stepping the photon energy through a preset range of values. The scan ranges used were 299.8–300.15 eV, 303.29–303.58 eV and 335.61–337.57 eV comprising the $[1s\,(2s\,2p)^3P]^2P^o$, $[1s\,(2s\,2p)^1P]^2P^o$ and the $[(1s\,2s)^3S\ 3p]^2P^o$ resonances, respectively. Each scan range consisted of 60 – 80 data points. The point-to-point step width was chosen according to the preselected experimental energy spread ΔE. The step width was 5 meV in the first two ranges and 25 meV in the third range.

The energy scale was calibrated by first applying a Doppler correction to account for the motion of the C^{3+} ions. The energy shift resulting from the monochromator calibration was determined by measurements of the photoions produced in photoionization of Ar gas in the vicinity of the Ar $2p_{3/2}$ edge and of CO gas in the vicinity of the C 1s edge. The Ar photoabsorption spectrum taken in the energy range 244 to 252 eV was compared with the measurements carried out by King *et al* [47] who employed electron-energy-loss spectroscopy (EELS) reaching unsurpassed precision in this energy range (10 meV at 244.39 eV). The present CO photoabsorption spectrum showing almost fully resolved vibrational excitations in CO was compared with the $1s \rightarrow \pi^*$ resonance energies measured by EELS [48] and with the relative resonance energies observed in CO photoexcitation [49] covering an energy range 287 to 306 eV. The precision of these measurements is at best 20 meV at 287.40 eV. The comparison of the present photoabsorption energies with the literature values showed deviations between 0.7 eV near 245 eV and 1.7 eV near 300 eV well represented by a linear increase with the monochromator's grating angle. This linear dependence was extrapolated all the way to 339 eV yielding a shift of about 2.5 eV. The set energies in the experiment were corrected by subtracting the energy shifts determined by the linear fit to the observed deviations. This procedure yields an uncertainty of ± 30 meV at 300 eV. Extrapolation of the calibration range to 340 eV, i.e., to the very end of the range of the monochromator grating, adds another ± 30 meV if the assumption of a linear dependence is correct. An estimate for the uncertainty of ± 100 meV at

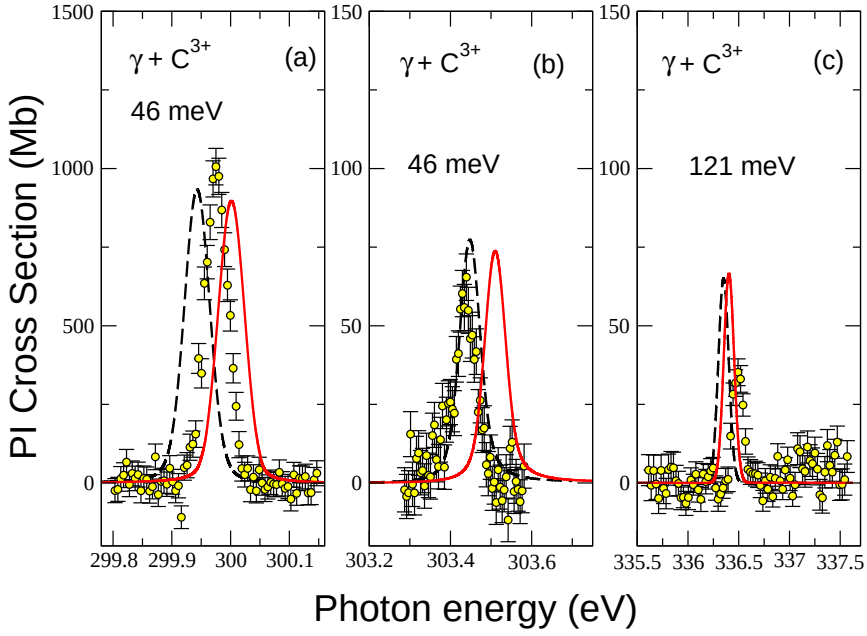


Figure 1. (Colour online) Absolute photoionization (PI) cross sections for K-shell ionization of Li-like C^{3+}: Experimental measurement from the ALS (symbols) and the R-matrix calculations with radiation damping (full lines, Breit-Pauli intermediate coupling, dashed lines LS coupling) convoluted with a FWHM Gaussian of the appropriate width) for (a) the $[1s\,(2s2p)^3P]^2P$ resonance, (b) the $[1s\,(2s2p)^1P]^2P$ resonance, and (c) the $[(1s\,2s)^3S\ 3p]^2P$ resonance. The experimental energy spreads obtained from the Voigt fits are (a) $\Delta E = 46$ meV, (b) $\Delta E = 46$ meV and (c) $\Delta E = 121$ meV.

340 eV appears to be more realistic.

4. Results and Discussion

The experimental K-shell photoionization (PI) cross sections for the C^{3+} ion are shown in figure 1. The full line is the result from the R-matrix calculations including radiation damping and convolution at the appropriate experimental resolution. This convolution masks asymmetric line shapes which become evident when zooming in to the cross section range 0 - 1 Mb. Experimental results for photoionization resonance strengths, level energies and, where possible, for Lorentzian widths of the first three Auger states were extracted from Voigt line profiles obtained from nonlinear least-squares fits to the measured data. The results from these fits are presented in table 1. Table 1 also displays the corresponding results of the present R-matrix calculations in addition to those from the most precise experimental and theoretical study to date of Mannervik et al. [45].

Mannervik and collaborators performed an electron-ion recombination experiment

Table 1. Comparison of PI resonance energies $E_{\rm ph}^{\rm (res)}$ (in eV), autoionization widths Γ (meV) and strengths $\overline{\sigma}^{\rm PI}$ (in Mb eV). The systematic uncertainty of the present experimental energy scale is 30 meV at 300 eV and an estimated 100 meV at 340 eV. On the basis of their thorough theoretical investigation of resonance energies the authors of reference [45] felt that the uncertainty of their energy scale was as low as 50 meV, however, this figure could not be derived strictly on experimental grounds. The systematic uncertainty of the present experimental cross sections is estimated to be 20% for the two resonances at lower energies and 40% for the third resonance. The related numbers for the associated PR resonances are not specified in reference [45]. For the comparison, the PR resonance strengths from reference [45] were converted by employing equation (1). The relative energies $E_{\rm ph}^{\rm (res)}(1)$ and $E_{\rm ph}^{\rm (res)}(2)$ of the first two resonances were determined in the experiment with a precision of 1 to 2 meV, from which a more accurate number for the energy splitting $\Delta E_{\rm res}$ (in eV) = $E_{\rm ph}^{\rm (res)}(2)$ - $E_{\rm ph}^{\rm (res)}(1)$ can be inferred.

Resonance		ALS (Expt)	R-matrix (Theory)	CRYRING (Expt)	SPM (MCDF) (Theory)
$[1s(2s2p)^3P]^2P^o$	$E_{\rm ph}^{\rm (res)}$ (1)	299.98 ± 0.03	299.99‡ 299.94†	299.98 ± 0.05	299.99*
	Γ	–	9.5‡ 9.5†	–	3.88* 9.5§
	$\overline{\sigma}^{\rm PI}$	53 ± 2	53.3‡ 54.4†	52.6 ± 0.8	–
$[1s(2s2p)^1P]^2P^o$	$E_{\rm ph}^{\rm (res)}$ (2)	303.44 ± 0.03	303.50‡ 303.43†	303.48 ± 0.05	303.46*
	Γ	27 ± 5	26.0‡ 25.6†	–	39.91* 25.4§
	$\overline{\sigma}^{\rm PI}$	4.5 ± 0.7	5.6‡ 5.8†	6.5 ± 0.4	–
$[(1s\,2s)^3S\ 3p]^2P^o$	$E_{\rm ph}^{\rm (res)}(3)$	336.50 ± 0.10	336.39‡ 336.33†	336.36 ± 0.05	336.39*
	Γ	–	0.13‡ 0.13†	–	0.55* 0.13§
	$\overline{\sigma}^{\rm PI}$	4.5 ± 0.9	8.6‡ 8.5†	7.0 ± 0.4	–
Energy splitting	$\Delta E_{\rm res}$	3.461± 0.004	3.509‡ 3.499†	3.50	3.465*

‡Breit-Pauli semi-relativistic intermediate coupling R-matrix (31-state).
†Non-relativistic LS coupling R-matrix (19-state).
*Saddle-Point-Method [45].
§MCDF method [50].

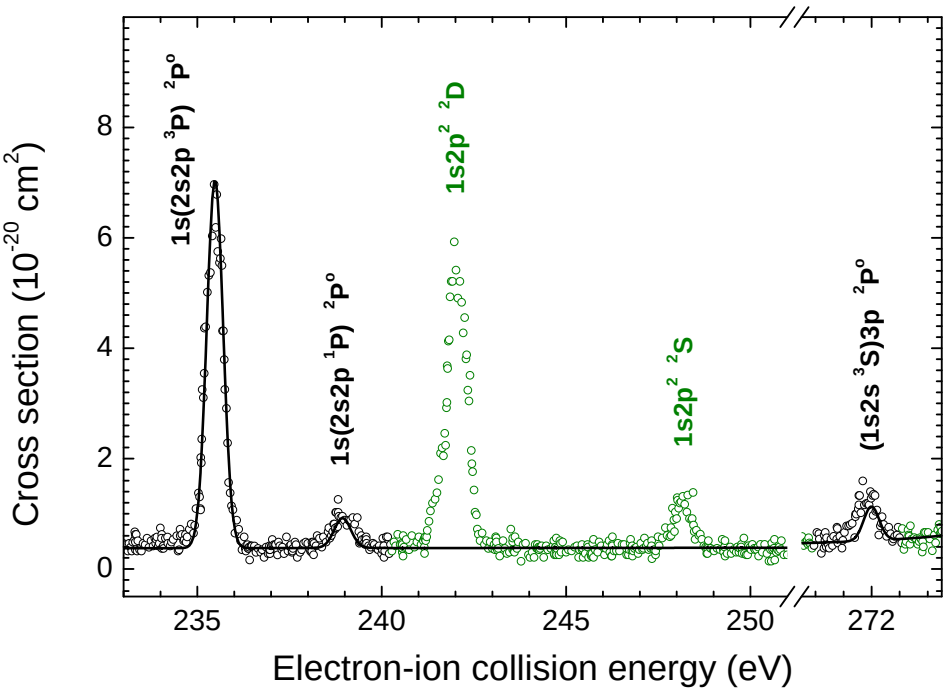


Figure 2. (Colour online) Absolute cross sections for the photorecombination (PR) of He-like C^{4+}. Comparison between the experimental C^{4+} PR results of Mannervik et al. [45] (open symbols) from the CRYRING and the present experimental C^{3+} photoionization (PI) results (full line) from the ALS. For comparison purposes the ALS PI cross-sections were converted into PR cross-sections (via equation 1) and convoluted with an appropriate Gaussian to account for the energy spread of the CRYRING PR experiment. The $[(1s\,2s)^3S\ 3p]^2P$ resonance is on the tail of a stronger PR-resonance at higher energies (not shown). The $1s^2\,2p\ ^2D$ and $1s^2\,2p\ ^2S$ resonances (open green circles) are only observed in the PR experiment since their photoexcitation from the ground state of C^{3+} is not dipole allowed.

with a cooled ion beam at a heavy-ion storage-ring [45, 46], and observed doubly excited C^{3+} resonance states in photorecombination (PR) of C^{4+} ions (figure 2). Photorecombination of C^{4+} is the time-reversed process of C^{3+} PI. The corresponding cross sections $\sigma^{\rm PR}$ and $\sigma^{\rm PI}$ can be compared on a state-to-state level [22, 51, 52] by employing the principle of detailed balance:

$$\sigma^{\rm PR}_{f\to i} = \sigma^{\rm PI}_{i\to f}\,\frac{g_i}{g_f}\,\frac{E^2_{\rm ph}}{2m_e c^2 E_e} \qquad (1)$$

Here $g_i = 2$ is the statistical weight of the $C^{3+}(1s^2\,2s\ ^2S_{1/2})$ ground state (labelled i), $g_f = 1$ is the statistical weight of the $C^{4+}(1s^2\ ^1S_0)$ ground state (labelled f). The PR and PI energy scales (denoted as $E_{\rm ph}$ and E_e, respectively) differ by the C^{3+} 2s-ionization energy $I_i = 64.49390$ eV [39], i. e. $E_e = E_{\rm ph} - I_i$.

Photorecombination generally leads to a multitude of final states. In the case of the 1s 2s np resonances, however, it may be assumed that only the radiative transition to the $1s^2\,2s$ ground state leads to a final state that is stable against autoionization.

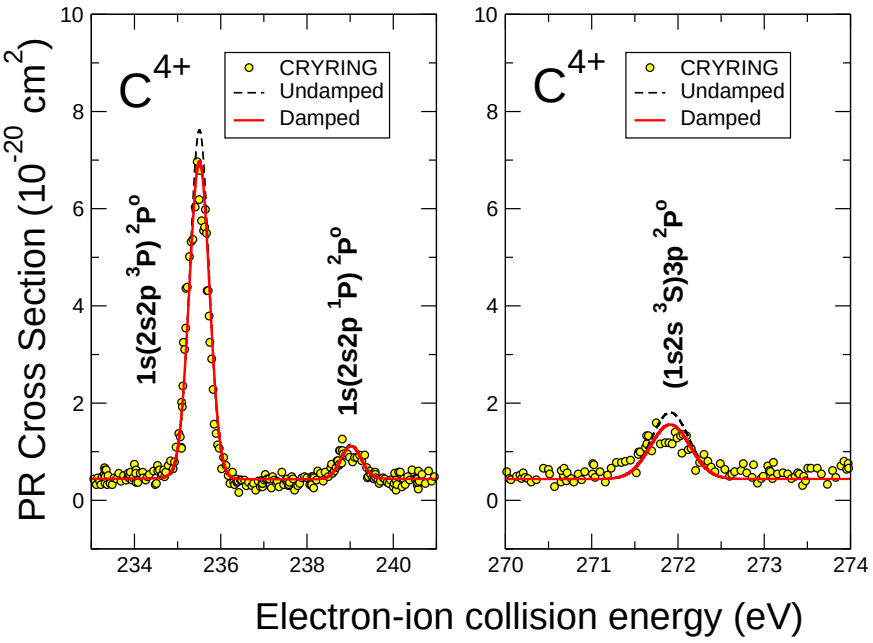


Figure 3. (Colour online) Absolute cross sections for the photorecombination (PR) of He-like C^{4+}. Comparison between the experimental C^{4+} PR results of Mannervik et al. [45] (open symbols) from the CRYRING and the present theoretical C^{3+} results from the 31-state intermediate coupling R-matrix method (full line, with radiation damping, dashed line, without radiation damping). Here again for comparison purposes the R-matrix PI cross sections were converted into PR cross sections (via equation 1) and convoluted with an appropriate Gaussian to account for the energy spread of the CRYRING PR experiment.

Therefore, the application of equation 1 facilitates a direct comparison of the resonance parameters obtained from the present PI experiment with the ones from the PR experiment.

For the comparison presented in figure 2 the present experimental PI cross sections were converted into PR cross sections (via equation 1) and convoluted with a Gaussian to account for the experimental energy spread ΔE of the PR experiment. The latter was determined from a fit of the converted PI cross section to the experimental PR cross section (full line in figure 2). The fit delivered $\Delta E = 520 \pm 60$ meV, i. e., an order of magnitude larger than in the present PI experiment.

In the comparison of the converted PI results with the PR data, an overall cross section scale factor was allowed to vary in order to match the converted PI and the experimental PR cross-section scales. This factor was determined to be 0.93 ± 0.16, i.e., both cross-section scales agree with one another within an uncertainty of 16%. The actual observed deviation from unity is within the combined systematic uncertainties of both experiments. In reference [45] no systematic uncertainty for the cross section scale is provided, however, error bars of 20% are typical for storage ring recombination

Table 2. Autoionization (Γ_a) and radiative rates (Γ_r) with branching ratios η (%) for the $1s2\ell2\ell'$ resonance states of the C^{3+} ion. The present results are determined in LS coupling. The MCDF calculations taken from reference [50] were averaged over fine-structure levels. The theoretical results from the Saddle-Point-Method (SPM) were taken from reference [45]. The numbers in the square brackets denotes the power of 10 by which the preceding term is to be multiplied.

$C^{3+}(1s2\ell2\ell')$ States	Present	Present	Other Methods	Other Methods
	Γ_a (meV, s^{-1})	Γ_r (meV, s^{-1})	Γ_a (meV, s^{-1})	Γ_r (meV, s^{-1})
$[1s(2s2p)^3P]^2P^o$	9.5, 1.44[13]	0.430, 6.54[11]	9.50, 1.43[13]† 3.88, 0.59[13]‡	0.322, 4.89[11]† 0.442, 6.72[11]‡
$[1s(2s2p)^1P]^2P^o$	25.6, 3.89[13]	0.057, 8.70[10]	25.40, 3.86[13]† 39.91, 6.07[13]‡	0.063, 9.57[10]† 0.049, 7.41[10]‡
$[(1s\,2s)^3S\ 3p]^2P^o$	0.133, 2.02[11]	0.087, 1.33[11]	0.127, 1.93[11]† 0.550, 8.36[11]‡	0.082, 1.25[11]† 0.086, 1.30[11]‡
			η (%)	
		$[1s(2s2p)^3P]^2P^o$	$[1s(2s2p)^1P]^2P^o$	$[(1s\,2s)^3S\ 3p]^2P^o$
$\Gamma_r/(\Gamma_a+\Gamma_r)$	Radiative	4.32§ 3.28† 10.20‡	0.22§ 0.25† 0.12‡	36.67§ 39.23† 13.50‡
$\Gamma_a/(\Gamma_a+\Gamma_r)$	Autoionization	95.68§ 96.72† 89.80‡	99.78§ 99.75† 99.88‡	63.33§ 60.77† 86.50‡

§Present LS coupling work.
†MCDF method [50].
‡Saddle-Point-Method (SPM) [45].

experiments and have been assumed here as well.

A closer inspection of the individual resonance strengths (table 1) highlights the agreement between the cross-section scales of the PI and PR experiments, especially for the strongest $[1s(2s2p)^3P]^2P^o$ resonance. The error bars for the integrated resonance strengths are statistical only. The ratios between the individual strengths from reference [45] and the present ones are 0.992, 1.44 and 1.56 in the order of table 1. Obviously there is less agreement for the weaker $[1s(2s2p)^1P]^2P^o$ and $[(1s\,2s)^3S\ 3p]^2P^o$ resonances. This might partly be attributed to the fact that in addition to the $1s^2\ 2s\ ^2S$ ground state there are more final states available for dielectronic recombination (DR)

via the $[1s(2s2p)^1P]^2P^o$ and $[(1s\,2s)^3S\ 3p]^2P^o$ resonances.

Both experiments agree with each other within the systematic uncertainties (30 meV for the present PI experiment and 50 meV for the PR experiment) for the $[1s(2s2p)^3P]^2P^o$ and $[1s(2s2p)^1P]^2P^o$ resonance energies. The present experimental resonance energies are lower by 4 meV and 44 meV, respectively, than those from reference [45]. The agreement with the theoretical results from reference [45] is excellent with differences of only 14 meV and 19 meV, respectively. The present intermediate coupling R-matrix calculations yield $[1s(2s2p)^3P]^2P^o$ and $[1s(2s2p)^1P]^2P^o$ resonance energies of 299.991 eV and 303.500 eV which are respectively 15 meV and 64 meV higher than our experimental values; 11 meV and 20 meV, compared to the CRYRING experiment. It is interesting to compare the energy difference $\Delta E_{res} = E_{\rm ph}^{\rm (res)}(2)$ - $E_{\rm ph}^{\rm (res)}(1)$ found in the ALS experiment (see entry $\Delta E_{\rm res}$ in table 1). The SPM approach is within the experimental uncertainty of the ALS experiment. The present intermediate coupling R-matrix calculations differ by only 10 meV from the *LS* R-matrix result, which again differs by 38 meV from the ALS result. We note that from earlier dielectronic recombination (DR) measurements taken at 2 eV resolution at the TSR storage ring in Heidelberg, Germany [53] less accurate results (compared to the present experimental values of 299.976 ± 0.03 eV and 303.436 ± 0.03 eV) of 298.794 ± 0.1 eV and 302.293 ± 0.3 eV, respectively, were obtained, as were theoretical predictions of 299.3 eV and 302.28 eV made by Pradhan and co-workers [34, 35] using the Breit-Pauli R-matrix method for the energies of these same resonances. The theoretical results of the Saddle-Point-Method (SPM) were taken from reference [45] and the MCDF values are from reference [50] averaged over fine-structure levels. From figure 1 and table 1 we see that the non-relativistic R-matrix results for the energies of all three resonances yield consistently lower values compared to those from more sophisticated theoretical approaches (which include relativistic effects) and with experiment. The autoionization linewidths and resonance strengths are of similar magnitude to the intermediate coupling R-matrix results. We note that the energy position of the $[1s(2s2p)^1P]^2P^o$ broad resonance from the *LS* coupling results is in better agreement with the ALS experiment.

The present experimental value of 336.492 ± 0.1 eV for the $[(1s\,2s)^3S\ 3p]^2P^o$ resonance position has a deviation of 132 meV between the ALS work and the value of 336.36 ± 0.05 eV from that of the CRYRING [45]. This we attribute to a deficiency of the present experimental energy calibration. The resonance energy of 336.4 eV is well outside the energy range where calibration lines were measured with an uncertainty of ± 30 meV (section 3). The extrapolation of the present calibration to energies well outside the investigated range introduces additional uncertainties that were estimated to result in a possible 0.1 eV error. The present intermediate coupling R-matrix value of 336.393 eV for the energy position of this resonance lies 33 meV above the experimental value from the CRYRING and thus still within its 50 meV experimental uncertainty.

Table 2 presents our *LS* results for the autoionization (Γ_a), radiative (Γ_r) rates and branching ratios (η) for the above three $1s2\ell2\ell'$ resonance states of C^{3+} together with results from the multi-configuration-Dirac-Fock (MCDF) approach [50] and the saddle point method [45]. We note from table 2 that our *LS* results for these quantities show better accord with the MCDF results [50] than with those from the saddle-point-method [45] and that inclusion of radiation damping in the R-matrix calculations will only affect the two narrow resonances observed in both the ALS and CRYRING spectra. This is illustrated clearly in figure 3 where it is seen

that radiation damping only affects the theoretical R-matrix results for the narrow resonances present in the PR cross sections. Finally, the good agreement of the present PI converted intermediate coupling R-matrix results with the PR experimental data (figure 3) obtained at the CRYRING by Mannervik and co-workers [45], provides further confidence in our present work.

5. Conclusion

State-of-the-art theoretical and experimental methods were used to study the photoionization of C^{3+} ions in the energy region near to the K-edge. Overall, agreement is found between the present theoretical and experimental results both on the photon-energy scale and on the absolute PI cross-section scale for this prototype Li-like system.

The strength of the present study is in its excellent experimental resolving power coupled with state-of-the-art theoretical predictions. The experimental energy resolution of 46 meV in the present work made possible a determination of the autoionization linewidth of the $[1s(2s2p)^1P]^2P^o$ resonance. The Voigt line-profile fit for this resonance yielded a value for the autoionization linewidth of 27 ± 5 meV which is in good agreement with the present theoretical prediction of 26 meV (table 1) and nearly 50% smaller than the theoretical result of Mannervik *et al* [45]. The energy resolution and calibration of the present PI experiment also made possible to determine the energy difference $\Delta E_{\rm res}$ between the C^{3+} ($[1s\,(2s\,2p)^1P]^2P^o$) and C^{3+} ($[1s\,(2s\,2p)^1P]^2P^o$) resonances with an uncertainty of only 4 meV. The difference $\Delta E_{\rm res} = 3.461 \pm 0.004$ eV is in agreement with the theoretical result of the saddle point method used by Mannervik *et al* [45].

The principle of detailed balance was used to compare the present PI cross-section measurements with previous experimental and theoretical cross sections for the time-inverse photo-recombination (PR) processes. This provides a valuable check between entirely different approaches for obtaining atomic cross sections on absolute scales and gives confidence in the accuracy of the results.

Acknowledgments

We acknowledge support by Deutsche Forschungsgemeinschaft under project number Mu 1068/10, by the US Department of Energy (DOE) under contract DE-AC03-76SF-00098 and grant DE-FG02-03ER15424, through PAPIIT IN108009 UNAM, and through NATO Collaborative Linkage grant 976362. We thank Sven Mannervik for providing the numerical data of the Stockholm C^{4+} recombination measurements. B M McLaughlin acknowledges support by the US National Science Foundation through a grant to ITAMP at the Harvard-Smithsonian Center for Astrophysics.

[1] McLaughlin B M 2001 *Spectroscopic Challenges of Photoionized Plasma* (*ASP Conf. Series* vol **247**) ed Ferland, G and Savin D W (San Francisco, CA: Astronomical Society of the Pacific) p 87

[2] Schneider D, Bruch R, Schwarz W H E, Chang T C and Moore C F 1977 *Phys. Rev. A* **15** 926

[3] Hofmann G, Müller A, Tinschert K and Salzborn E 1990 *Z. Phys. D: Atoms, Molecules and Clusters* **16** 113

[4] Jannitti E, Nicolosi P, Villoresi P and Xianping F 1995 *Phys. Rev. A* **51** 314

[5] Schlachter A S, Sant'Anna M M, Covington A M, Aguilar A, Gharaibeh M F, Emmons E D, Scully S W J, Phaneuf R A, Hinojosa G, Álvarez I, Cisneros C, Müller A and McLaughlin B M 2004 *J. Phys. B: At. Mol. Opt. Phys.* **37** L103

[6] Scully S W J, Aguilar A, Emmons E D, Phaneuf R A, Halka M, Leitner D, Levin J C, Lubell M S, Püttner R, Schlachter A S, Covington A M, Schippers S, Müller A and McLaughlin B M 2005 *J. Phys. B: At. Mol. Opt. Phys.* **38** 1967

[7] Kaastra J S and Mewe R 1993 *Astrophys. J. Suppl. Ser.* **97** 443

[8] Reilman R and Manson S T 1979 *Astrophys. J. Suppl. Ser.* **40** 815

[9] Verner D A, Yakovlev D G, Band I M and Trzhaskovskaya M B 1993 *At. Data Nucl. Data Tables* **55** 233

[10] Verner D A and Yakovlev D G 1995 *Astron. & Astrophys. Suppl.* **109** 125

[11] Ferland G J, Korista K T, Verner D A, Ferguson J W, Kingdon J B and Verner E M 1998 *Pub. Astron. Soc. Pac.(PASP)* **110** 761

[12] Ferland G J 2003 *Ann. Rev. of Astron. & Astrophys.* **41** 517

[13] Kallman T R and Bautista M A 2001 *Astrophys. J. Suppl. Ser.* **134** 139

[14] Sembach K R, Savage B D and Jenkins E B 1994 *Astrophys. J.* **421** 585

[15] Nieva M F and Przybilla N 2008 *Astron. & Astrophys.* **481** 199

[16] Kjeldsen H, Folkmann F, Hansen J E, Knudsen H, Rasmussen M S, West J B and Andersen T 1999 *Astrophys. J* **524** L143

[17] West J 2001 *J. Phys. B: At. Mol. Opt. Phys.* **34** R45

[18] West J 2004 *Rad. Phys. Chem.* **70** 275

[19] Kjeldsen H 2006 *J. Phys. B: At. Mol. Opt. Phys.* **39** R325

[20] Scully S W J, Álvarez I, Cisneros C, Emmons E D, Gharaibeh M F, Leitner D, Lubell M S, Müller A, Phaneuf R A, Püttner R, Schlachter A S, Schippers S, Ballance C P and McLaughlin B M 2006 *J. Phys. B: At. Mol. Opt. Phys.* **39** 3957

[21] Scully S W J, Álvarez I, Cisneros C, Emmons E D, Gharaibeh M F, Leitner D, Lubell M S, Müller A, Phaneuf R A, Püttner R, Schlachter A S, Schippers S, Ballance C P and McLaughlin B M 2007 *J. Phys. Conf. Ser.* **58** 387

[22] Müller A, Phaneuf R A, Aguilar A, Gharaibeh M F, Schlachter A S, Álvarez I, Cisneros C, Hinojosa G and McLaughlin B M 2002 *J. Phys. B: At. Mol. Opt. Phys.* **35** L137

[23] Müller A, Phaneuf R A, Aguilar A, Gharaibeh M F, Schlachter A S, Álvarez I, Cisneros C, Hinojosa G and McLaughlin B M 2003 *Nucl. Inst. & Methods B* **205** 301

[24] Schippers S, Müller A, McLaughlin B M, Aguilar A, Cisneros C, Emmons E D, Gharaibeh M F, Phaneuf R A 2003 *J. Phys. B: At. Mol. Opt.* **36** 3371

[25] Müller A, Schippers S, Phaneuf R A, Kilcoyne A L D, Bräuning H, Schlachter A S, Lu M and McLaughlin B M 2007 *J. Phys.: Conf. Ser.* **58** 383

[26] Covington A M, Aguilar A, Covington I R, Gharaibeh M F, Shirley C A, Phaneuf R A, Álvarez I, Cisneros C, Hinojosa G, Dominguez-Lopez I, Sant'Anna M M, Schlachter A S, McLaughlin B M and Dalgarno 2002 *Phys. Rev. A* **66** 062710

[27] Covington A M, Aguilar A, Covington I R, Gharaibeh M F, Shirley C A, Phaneuf R A, Álvarez I, Cisneros C, Hinojosa G, Bozek J D, Dominguez I, Sant'Anna M M, Schlachter A S, Berrah N, Nahar S N and McLaughlin B M 2001 *Phys. Rev. Lett.* **87** 243002

[28] Aguilar A, Covington A M, Hinojosa G, Phaneuf R A, Álvarez I, Cisneros C, Bozek J D, Dominguez I, Sant'Anna M M, Schlachter A S, Nahar S N and McLaughlin B M 2003 *Astrophys. J. Suppl. Ser.* **146** 467

[29] Aguilar A, Emmons E D, Gharaibeh M F, Covington A M, Bozek J D, Ackerman G, Canton S, Rude B, Schlachter A S, Hinojosa G, Álvarez I, Cisneros C, McLaughlin B M and Phaneuf R A 2005 *J. Phys. B: At. Mol. Opt. Phys.* **38** 343

[30] Burke P G and Berrington K A 1993 *Atomic and Molecular Processes: An R-matrix Approach* (Bristol, UK: IOP Publishing)

[31] Berrington K A, Eissner W and Norrington P H 1995 *Comput. Phys. Commun.* **92** 290 URL `http://amdpp.phys.strath.ac.uk/APAP`

[32] Cunto W, Mendoza C, Ochsenbein F and Zeippen C J 1993 *Astron. & Astrophys.* **275** L5

[33] McGuiness C, Bell K L and Hibbert A 1997 *J. Phys. B: At. Mol. Opt. Phys.* **30** 59

[34] Nahar S N and Pradhan A K 2001 *Phys. Rev. A* **63** 060701
[35] Pradhan A K, Chen, G X, Nahar S N and Zhang H L 2001 *Phys. Rev. Lett.* **87** 183201
[36] Robicheaux F, Gorczyca T W, Griffin D C, Pindzola M S and Badnell N R 1995 *Phys. Rev. A* **52** 1319
[37] Hibbert A 1975 *Comput. Phys. Commun.* **9** 141
[38] Clementi E and Roetti C 1974 *At. Data Nucl. Data Tables* **14** 177
[39] Ralchenko Y, Kramida A E, Reader J, and NIST ASD Team, NIST Atomic Spectra Database (version 3.1.4), National Institute of Standards and Technology, Gaithersburg, MD, USA URL `http://physics.nist.gov/asd3`
[40] Quigley L and Berington K A 1996 *J. Phys. B: At. Mol. Phys.* **29** 4529
[41] Quigley L, Berington K A and Pelan J 1998 *Comput. Phys. Commun.* **114** 225
[42] Ballance C P, Berington K A and McLaughlin B M 1999 *Phys. Rev. A* **60** R4217
[43] Lyon I C, Peart B, West J B and Dolder K 1986 *J. Phys. B: At. Mol. Phys.* **19** 4317
[44] Brötz F, Trassl R, McCullough R W, Arnold W and Salzborn E 2001 *Phys. Scr.* **T92** 278
[45] Mannervik S, Asp S, Broström L, DeWitt D R, Lidberg J, Schuch R and Chung K T 1997 *Phys. Rev. A* **55** 1810
[46] Mannervik S, DeWitt D R, Engström L, Lidberg J, Lindroth E, Schuch R and Zong W 1998 *Phys. Rev. Lett.* **81** 313
[47] King G C, Tronc M, Read F H, and Bradford R C 1977 *J. Phys. B: At. Mol. Phys.* **10** 2479
[48] Sodhi R N S and Brion C E 1977 *J. Electron Spectrosc. Relat. Phenom.* **34** 363
[49] Domke M, Xue C, Puschmann, Mandel T, Hudson E, Shirley D A and Kaindl G 1990 *Chem. Phys. Lett.* **173** 122
[50] Chen M H 1986 *At. Data Nucl. Data Tables* **34** 301
[51] Schippers S, Müller A, Ricz S, Bannister M E, Dunn G H, Bozek J D, Schlachter A S, Hinojosa G, Cisneros C, Aguilar A, Covington A M, Gharaibeh M F and Phaneuf R A 2002 *Phys. Rev. Lett.* **89** 193002
[52] Schippers S, Müller A, Phaneuf R A, van Zoest T, Álvarez I, Cisneros C, Emmons E D, Gharaibeh M F, Hinojosa G, Schlachter A S and Scully S W J 2002 *J. Phys. B: At. Mol. Opt. Phys.* **37** L209
[53] Kilgus G, Habs D, Schwalm D, Wolf A, Schuch R and Badnell N R 1993 *Phys. Rev. A* **47** 4859